DELINEATION OF GEOLOGICAL BOUNDARY IN IDI-EMI AND ENVIRONS, SOUTHWESTERN NIGERIA USING ELECTRICAL RESISTIVITY METHOD

S. A. Adekoya [1,*]
J. O. Coker [1]
H. T. Oladunjoye [1]
O. A. Adenuga[1]
F. O. Ogunsanwo[2]
A. A. Alabi[3]
P. A. Adesanya[1]

Received: 04/08/2025
Revised: 12/09/2025
Accepted: 13/09/2025

[1] Department of Physics, Faculty of Science, Olabisi Onabanjo University, Ago-Iwoye.
[2] Department of Physics, Faculty of Science, Tai Solarin University of Education Ijagun, Ijebu-Ode
[3] Department of Physics, Faculty of Science, Federal University of Agriculture, Abeokuta
*Corresponding Author's Email: adekoya.sofiat@oouagoiwoye.edu.ng

DELINEATION OF GEOLOGICAL BOUNDARY IN IDI-EMI AND ENVIRONS, SOUTHWESTERN NIGERIA USING ELECTRICAL RESISTIVITY METHOD

Adekoya, Sofiat A
Department of Physics, Faculty of Science, Olabisi Onabanjo University, Ago-Iwoye.
adekoya.sofiat@oouagoiwoye.edu.ng

Coker, Joseph O
Department of Physics, Faculty of Science, Olabisi Onabanjo University, Ago-Iwoye.
coker.joseph@oouagoiwoye.edu.ng

Oladunjoye, Hamid T
Department of Physics, Faculty of Science Olabisi Onabanjo University, Ago-Iwoye.
oladunjoye.hamid@oouagoiwoye.edu.ng

Adenuga, Omolara A
Department of Physics, Faculty of Science Olabisi Onabanjo University, Ago-Iwoye.
adenuga.omolara@oouagoiwoye.edu.ng

Ogunsanwo, Fidelis O
Department of Physics, Faculty of Science Tai Solarin University of Education Ijagun, Ijebu-Ode
godif07@yahoo.com

Alabi, Aderemi A
Department of Physics, Faculty of Science, Federal University of Agriculture, Abeokuta
derylab@yahoo.com

Adesanya, Paula A
Department of Physics, Faculty of Science, Olabisi Onabanjo University Ago-Iwoye
adesanyapaula019@gmail.com.

***Abstract*—** Old geological maps in areas with complex rock formations often lack accuracy, risking misinformation, especially where lithological boundaries are subtle. This study integrates Vertical Electrical Sounding (VES) and 2D electrical imaging to improve subsurface mapping in the Idi-Emi area, southwestern Nigeria. The approach successfully identified three terrain types—sedimentary, transition, and basement complex—each with distinct resistivity and layer thickness ranges. The topmost geoelectric layers showed resistivities of 42–634 Ωm and thicknesses of 0.6–1.9 m across these terrains. New geological boundaries were delineated, refining the existing map and aligning with the Dahomey Basin framework. The enhanced geological model provides critical insights for groundwater aquifer delineation, hydrogeological exploration, and controlling illegal mining activities in the region. This integrated geophysical method demonstrates a valuable approach for accurate subsurface characterisation in geologically complex terrains.

Keywords— Geological Boundary, Basin, Lithostratigraphy, Transition Zone, Inhomogeneous Rocks

I. INTRODUCTION

Geophysical techniques involve the measurement of signals resulting from natural or artificial occurrences involving physical properties of subsurface formations [1]. Geophysical methods discover variances or anomalies in physical qualities inside the Earth's crust by detecting variations in magnetic susceptibility, electrical resistivity, seismic velocity, density, and elasticity using minimal or non-intrusive instrumentation for quick data collection.

Applications of geophysical methods include mineral exploration [2], groundwater exploration [3] [4], detection of ancient artefacts [5] [6], and detection and monitoring of environmental contaminants [7]. [8] [9] and geological characterisation [10].

Geological maps are considered conventional forms of geographic data that show different stratified rock layers. The accuracy of geological maps is generally dependent on the quantity of outcrop exposures because they are often created using regional studies, field observations, drill record interpretation, and remotely sensed data [11] [12]. Results from the use of a single geophysical technique are less reliable due to the inherent shortcomings of individual geophysical procedures, even though the use of massive data sets has improved the precision of recent results obtained on geological mappings and the accuracy with which stratigraphic boundaries could be defined [13]. For instance, borehole data provide one-dimensional (1-D) delineation around a single point, probing laterally into the Earth's surface. Furthermore, information obtained through the analysis of remotely sensed data is very unreliable. Geological boundaries are routinely established based on inaccurate information [11] [12].

Historical maps in regions with heterogeneous rock types may be inaccurate and include serious potential errors, particularly in terrains with modest lithological variances that could make it challenging to establish relevant map units. Idi-Emi, the area of study, is situated in the eastern Dahomey Basin in southwestern Nigeria, distinguishing what is relevant in generating genuine geological map units difficult because of the complex nature of lithological variations within the Abeokuta Group. Furthermore, as new geological boundaries for regional maps are defined, there is a risk of defining incorrect units based on geographically minor lithological differences or of portraying broad areas as homogeneous, whereas little but persistent changes in features reflect different and varied depositional histories ([13]). The challenges of classifying available rocks and minerals, identifying the available mineral quantity for commercial purposes and enacting available laws that could stop illegal mining in Idi-Emi, coupled with recent revelations on rock inhomogeneity within large areas that were thought to have homogenous lithography, have called for a redefinition of its

geological boundary; as a result, a comprehensive geologic map of the area of study is required. The study aims at delineating the geological boundary of Idi-Emi, around Imeko-Afon, by delineating the underlying layers, their resistivities and thickness to determine the stratigraphy of the area of study. The study will also identify geological structures based on variances of the subsurface rock's electrical characteristics.

A. Geological and Geographical setting

This research study area is Idi-Emi, situated in the Imeko-Afon Local Council Development Area of Ogun State, Southwestern Nigeria. It lies within latitudes 6º 42′N to 7º 17′N and longitudes 3º 0′E to 3º 57′E. Minimum temperatures in the south vary from 19°C to 22°C, while maximum temperatures in the south range from 32°C to 35°C [14]. The region's average rainfall is 1200 mm, with a little decrease from south to north.

The study region is part of the Eastern Dahomey Basin, surrounded by basement rock in the north and sedimentary strata of the eastern Dahomey Basin in the south. The migmatite and granitic gneisses, quartzites, mildly migmatized to unmigmatized paraschists and meta-igneous rocks, charnockitic, gabbroic, and dioritic rocks, and members of the Older Granite suite, notably granite, granodiorites, and syenites, are the most common rocks found in this area [15] [16]. Dolerite dykes, the newest elements of this complex, cut through all of the other rocks in the vicinity, demonstrating strong contacts. The geographic view of Idi-Emi is shown in Fig. 1. The hypersthene-quartz diorite found in Idi-Emi has hypidiomorphic granular texture, greenish-brown color, and minerals that suggest charnockitic affinities [17] [18]. The rock differs from typical charnockitic 'intermediate members' in two ways: (i) (i) antiperthite is relatively sparsely developed, and (ii) orthopyroxene crystals lack the strong pleochroism seen in charnockitic hypersthenes [18].

II. METHODS

The electrical resistivity approach was applied to create a physical map of the site's subsurface, locate fracture zones, and collect data on the structural and physical attributes of the ground. The method utilizes current from a direct commutated or low-frequency alternating current of electromotive force to depict the Earth's content, and according to Ohm's Law, a proportional relationship exists between the resulting potential difference (V) between the potential electrode pair and the magnitude of current (I) transmitted via the current electrode, with the constant of proportionality of these two parameters being the resistance (R) of the Earth material along the path followed by the current. Resistivity of the Earth's materials, which is the ability of a material to impede (or resist) the flow of electrical current through it, is given in equation 1.

$$\rho = \frac{RA}{l} \quad (1)$$

The system international (SI) unit is Ωm. For the purpose of determining the distribution of resistivity in subsurface materials, and because of the challenging geology of the research area, the Vertical Electrical Sounding (VES) technique was utilized in this study to take measurements of the change in Earth's resistivity both vertically and horizontally. In general, resistivity is measured by sending current into the ground via two current electrodes, C1 and C2, and measuring the voltage difference between them by two potential electrodes, P1 and P2. Three (3) traverses were acquired at a maximum of 200 m long, as shown in the base map (Fig. 2). A total of 22 VES points were acquired along three traverses up to 200 meters in length. Electrical current was injected through current electrodes (C1 and C2), while potential differences were recorded via potential electrodes (P1 and P2). Field measurements were manually plotted on log-log graphs of apparent resistivity versus half-current electrode spacing (AB/2) and initially interpreted using curve-matching techniques.

To ensure data accuracy and model reliability, a comprehensive error analysis was integrated into the workflow. Repeat measurements were performed at selected AB/2 spacings to check for consistency. Variations greater than ±10% were flagged as potential outliers due to contact resistance or environmental noise. The resulting data was processed using Prosys II, allowing importation, validation, and transformation of the raw data into formats compatible with modeling software. The final inversion was conducted using a finite element inversion algorithm (WinResist), generating 1D resistivity models that reflect vertical resistivity variations. Root Mean Square (RMS) Error values were computed to assess the quality of fit between observed and calculated resistivity values. Models with RMS errors below 10% were considered acceptable as proposed by [19]. A sensitivity analysis was manually performed by varying resistivity and thickness parameters ±10–20% in selected layers to evaluate the effect on RMS error. Significant changes in misfit indicated well-constrained parameters, while minimal changes revealed potential non-uniqueness or poor resolution [20]. The final resistivity models were used to delineate distinct subsurface zones. Sedimentary terrains were characterized by low resistivity (10–2500 Ωm), basement complexes by high resistivity (>5000 Ωm), and transition zones by intermediate resistivity (100–5000 Ωm) [21] [22]; [20]. These interpretations guided the identification of structural complexities, lithological changes, and geologic boundaries, which are relevant to groundwater exploration, engineering site investigation, and land-use planning.

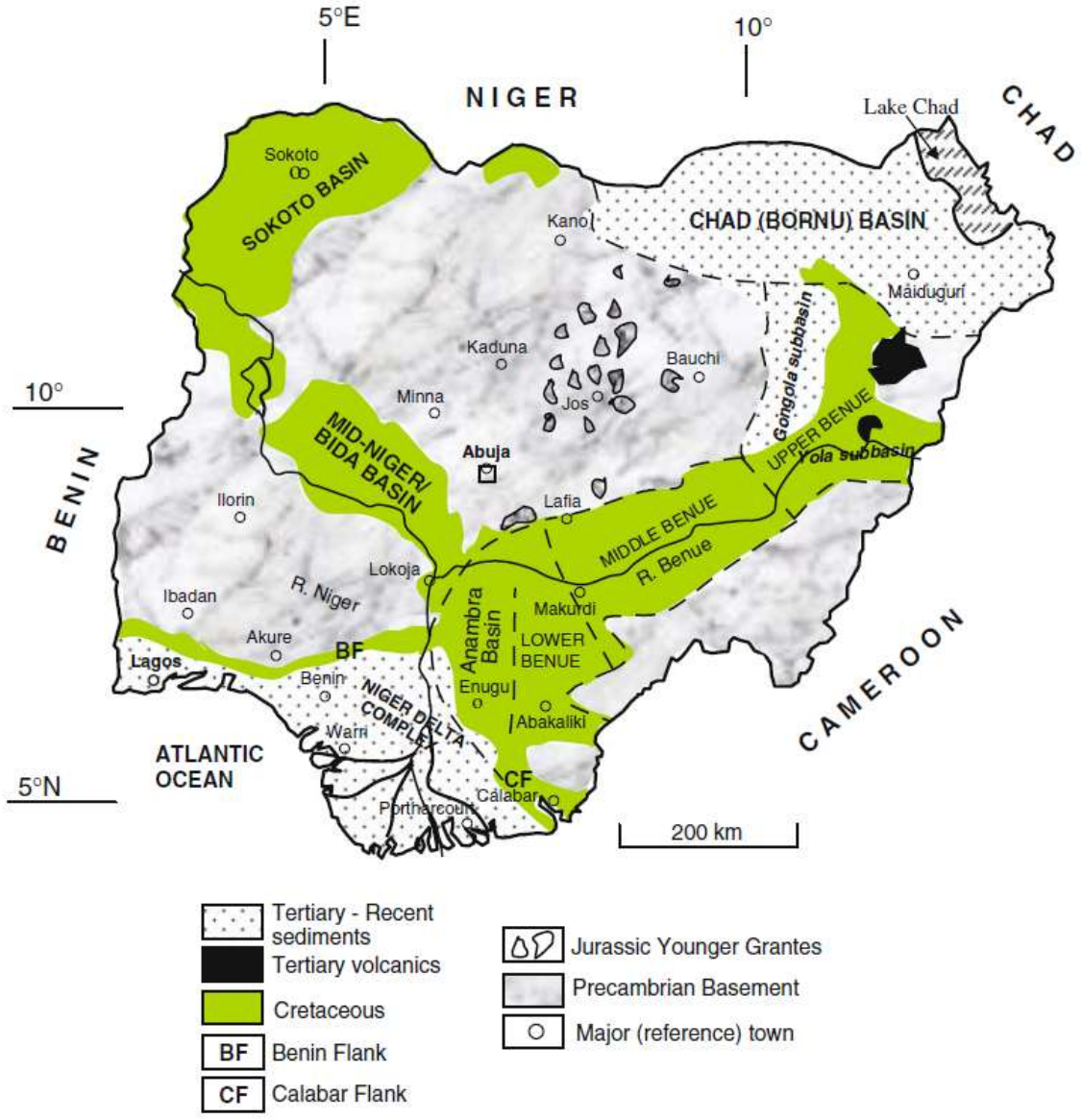

Figure. 1: Nigeria's Geographical Map (adapted from [23]

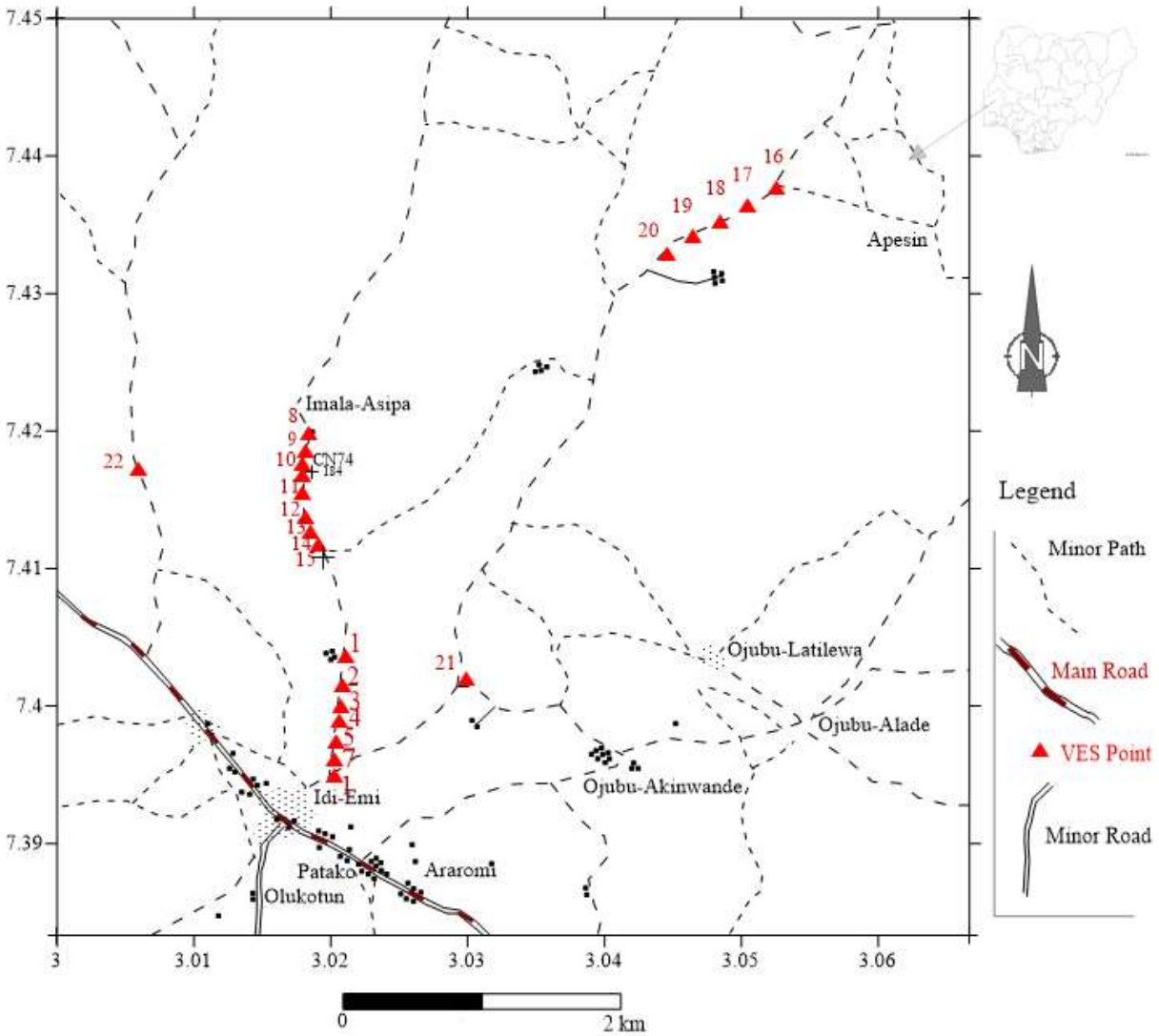

Figure. 2: The Base map showing VES profiles at Idi-Emi

III. Results

Table 1 summarizes the Vertical Electrical Sounding (VES) results, including resistivity, thickness, depth, curve types, lithological interpretations, and inferred terrain. Eight distinct resistivity curve types were identified across the study area—H, AA, HA, AK, HK, KH, KHK, and HKH—each reflecting underlying geological variations. The H and HKH types are predominant in the northern and southwestern margins, respectively; KH occurs mainly in the central region, while the remaining curve types are characteristic of the southern portion. Representative resistivity curves are illustrated in Figs. 3 to 6. Apparently, the resistivity curves generally revealed a range of three (3) to five (5) geo-electric layers. From the parameters of iterations (resistivity value, thickness, and depth) associated with the individual curve, the boundary line across the major geologic provinces is drawn.

Table1: Summary of VES result for Sedimentary terrain

VES STATION	LAYER NUMBER	RESISTIVITY (Ωm)	THICKNESS (m)	DEPTH (m)	CURVE TYPE	LITHOLOGIC INFERENCE	INFERRED TERRAIN
1	1	500	0.6	0.6		Topsoil	
	2	530	3.1	3.7	AA	Kaolinitic Sand	Sedimentary
	3	1500	36.3	40		Sand	
	4	2000	-			Dry Sand	
2	1	248	0.9	0.9		Topsoil	
	2	187	1.4	2.3	HA	Sandy Clay	Sedimentary
	3	917	54	56.3		Sand	
	4	1685	-	-		Dry Sand	
3	1	537	0.9	0.9		Topsoil	
	2	267	5.5	6.5	HA	Clayey Sand	Sedimentary
	3	871	44.6	51.1		Sand	
	4	2998	-	-		Dry Sand	
4	1	180	0.8	0.8		Topsoil	
	2	289	4.6	5.4	AA	Clayey Sand	Sedimentary
	3	1188	45.5	50.8		Sand	
	4	2102	-	-		Dry Sand	
5	1	634	0.8	0.8		Topsoil	
	2	900	8.2	9	AK	Kaolinitic Sand	Sedimentary
	3	2400	56	65		Dry Sand	
	4	1840	-	-		Wet Sand	
6	1	238	0.9	0.9		Topsoil	
	2	707	5.3	6.2	AK	Kaolinitic Sand	Sedimentary
	3	2664	54.3	60.5		Dry Sand	
	4	1331	-	-		Wet Sand	
7	1	42	1.2	1.2		Topsoil	
	2	188	3.6	4.8	AK	Sandy Clay	Sedimentary
	3	3038	51.5	56.3		Dry Sand	
	4	756	-	-		Wet Sand	

Table2: Summary of VES result for Transition terrain

VES STATION	LAYER NUMBER	RESISTIVITY (Ωm)	THICKNESS (m)	DEPTH (m)	CURVE TYPE	LITHOLOGIC INFERENCE	INFERRED TERRAIN
8	1	1043	1.2	1.2		Topsoil	
	2	49	19.2	20.4		Clay	Transition zone
	3	857	57.2	77.6	HK	Fresh Basement	
	4	302	-	-		Fractured Basement	
9	1	120	0.8	0.8	KH	Topsoil	Transition zone
	2	205	2	2.8		Lateritic Clay	
	3	33	13.1	15.9		Clay	
	4	915	-	-		Fresh Basement	
10	1	153	1.2	1.2		Topsoil	
	2	180	4.8	6	KH	Lateritic Clay	Transition zone
	3	80	29	35		Clay	
	4	630	-	-		Fresh Basement	
11	1	315	0.9	0.9		Topsoil	
	2	1200	9.1	10	KH	Kaolinitic Sand	Transition zone
	3	330	48	58		Clayey Sand	
	4	1500	-	-		Fresh Basement	
12	1	2240	0.8	0.8		Topsoil	
	2	3900	7.2	8		Conglomeratic Sand	Transition zone
	3	2701	15.5	23.5	KHK	Conglomeratic Clay	
	4	3699	23	46.5		Conglomeratic Sand	
	5	471	-	-		Clayey Sand	
13	1	2699	0.8	0.8		Topsoil	
	2	5513	3.1	3.9		Conglomeratic Sand	Transition zone
	3	2891	9	12.9	KHK	Kaolinitic Sand	
	4	5688	50.8	63.7		Conglomeratic Sand	
	5	1893	-	-		Wet Gravel/Sand	
							Transition zone
14	1	2855	0.8	0.8		Topsoil	
	2	5308	2.8	3.6		Conglomeratic Sand	Transition zone
	3	1781	11.3	14.9	KHK	Kaolinitic sand	
	4	11664	59.5	74.4		Conglomeratic Sand	
	5	3124	-	-		Wet Gravel/Sand	
15	1	1623	0.8	0.8		Topsoil	
	2	3270	2.4	3.1		Conglomeratic Sand	Transition zone
	3	1844	11	14.1		Kaolinitic Sand	
	4	11615	70.6	84.7	KHK	Conglomeratic Sand	
	5	4244	-	-		Wet Gravel/Sand	

IV. Discussion

Sedimentary Terrain

Traverse 1 was generated using the geoelectric sections of VES1-7 as shown in Fig. 7, which falls within the sedimentary terrain at Idi-Emi. The topmost geo-electric layer possesses a resistivity and thickness range of 42 Ωm – 634 Ωm and 0.6 m – 1.2 m. It is inferred as the topsoil. Resistivity components of this layer widely revealed a sandy topsoil with minor pockets of clay. Underlying the topsoil is a highly heterogeneous geo-electric stratum composed of resistivity units varying between 530 Ωm – 900 Ωm, 267 Ωm – 289 Ωm, and 187 Ωm – 188 Ωm (Fig. 7), respectively interpreted as kaolinitic sand, clayey sand, and sandy clay. It is majorly a kaolinitic and clayey sand layer embedded with minor lenses of sandy clay. The thickness range of the layer is 1.4 m – 8.2 m. Beneath the heterogeneous geo-electric layer lies a fairly homogeneous stratum with a resistivity range of 871 Ωm – 3038 Ωm and thickness ranges between 36.3 m and 56.0 m; it is inferred as a sand stratum. Due partly to increasing geothermal gradient with depth along VES 1, 2, 3, and 4, the sand stratum became more resistive, exhibiting a resistivity range of 1685 Ωm – 2998 Ωm, and inferentially reflecting a dry sand stratum. This is, however, not the case beneath VES 5, 6, and 7, which experienced a drastic drop in resistivity value to a range of 756 Ωm – 1840 Ωm due to groundwater circulation. The lithologic inference for this unit is wet sand. Around the Ogene axis (VES 21), four geo-electric units with resistivity values of 180 Ωm, 320 Ωm, 121 Ωm, and 289 Ωm were revealed from top to bottom (shown in Fig. 8). By inference, the unit corresponds to a 0.9 m–thick topsoil, 8.5 m–thick clayey sand, 50.5 m–thick sandy clay, and fractured basement in the aforementioned order. Cumulative thickness of the strata on the fractured basement is 59.9 m. This axis is another notable transition zone between the basement complex and the continental margin of the Eastern Dahomey Basin.

Table 3: Summary of VES result for Basement terrain

VES STATION	LAYER NUMBER	RESISTIVITY (Ωm)	THICKNESS (m)	DEPTH (m)	CURVE TYPE	LITHOLOGIC INFERENCE	INFERRED TERRAIN
16	1	1071	1.1	1.1		Topsoil	
	2	59	25.8	26.9		Clay	
	3	1231	52.7	79.6	HK	Fresh Basement	Basement
	4	202	-	-		Fractured Basement	
17	1	638	1.9	1.9		Topsoil	
	2	117	20.1	22	H	Sandy Clay	Basement
	3	1044	-	-		Fresh Basement	
18	1	1105	1	1		Topsoil	
	2	100	5.6	6.6		Sandy Clay	
	3	393	10.5	17.1	HKH	Clayey Sand	
	4	65	23	40.1		Fractured Basement	Basement
	5	1602	-	-		Fresh Basement	
19	1	2015	1.7	1.7		Topsoil	
	2	56	8.3	10		Clay	
	3	168	12.8	22.8	HKH	Sandy Clay	Basement
	4	26	31.3	54.2		Fractured Basement	
	5	1421	-	-		Fresh Basement	
20	1	338	0.9	0.9		Topsoil	
	2	60	14.1	15	H	Clay	Basement
	3	2659	-	-		Fresh Basement	
21	1	145	0.9	0.9		Topsoil	
	2	320	8.5	9.4	KH	Clayey Sand	
	3	121	50.5	59.9		Sandy Clay	Sedimentary
22	1	102	1.4	1.4		Topsoil	
	2	25	17.1	18.5	KH	Clay	Basement
	3	943	-	-		Fresh Basement	

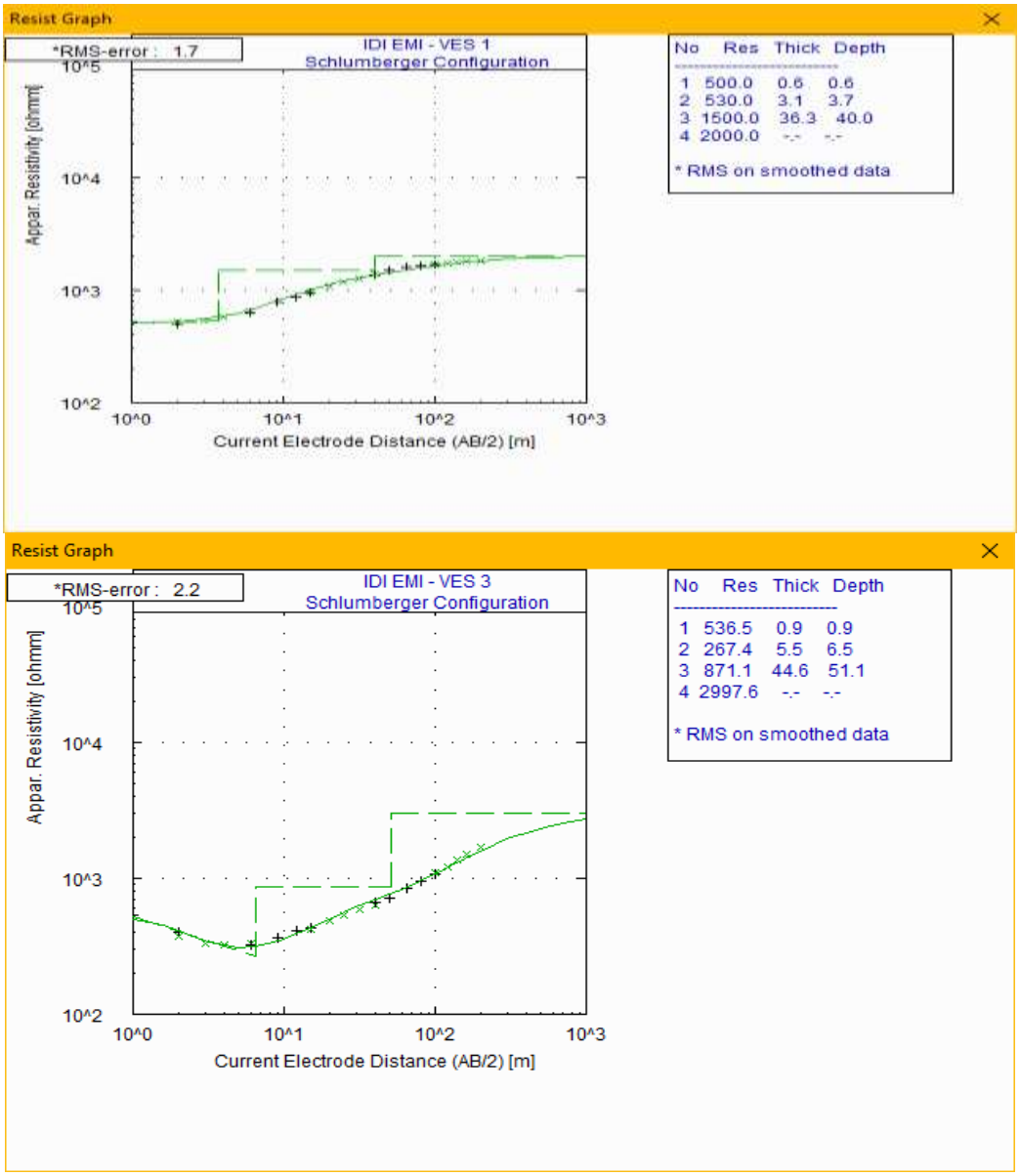

Figure. 3: a) Resistivity model for curve type AA b) resistivity model for curve type HA

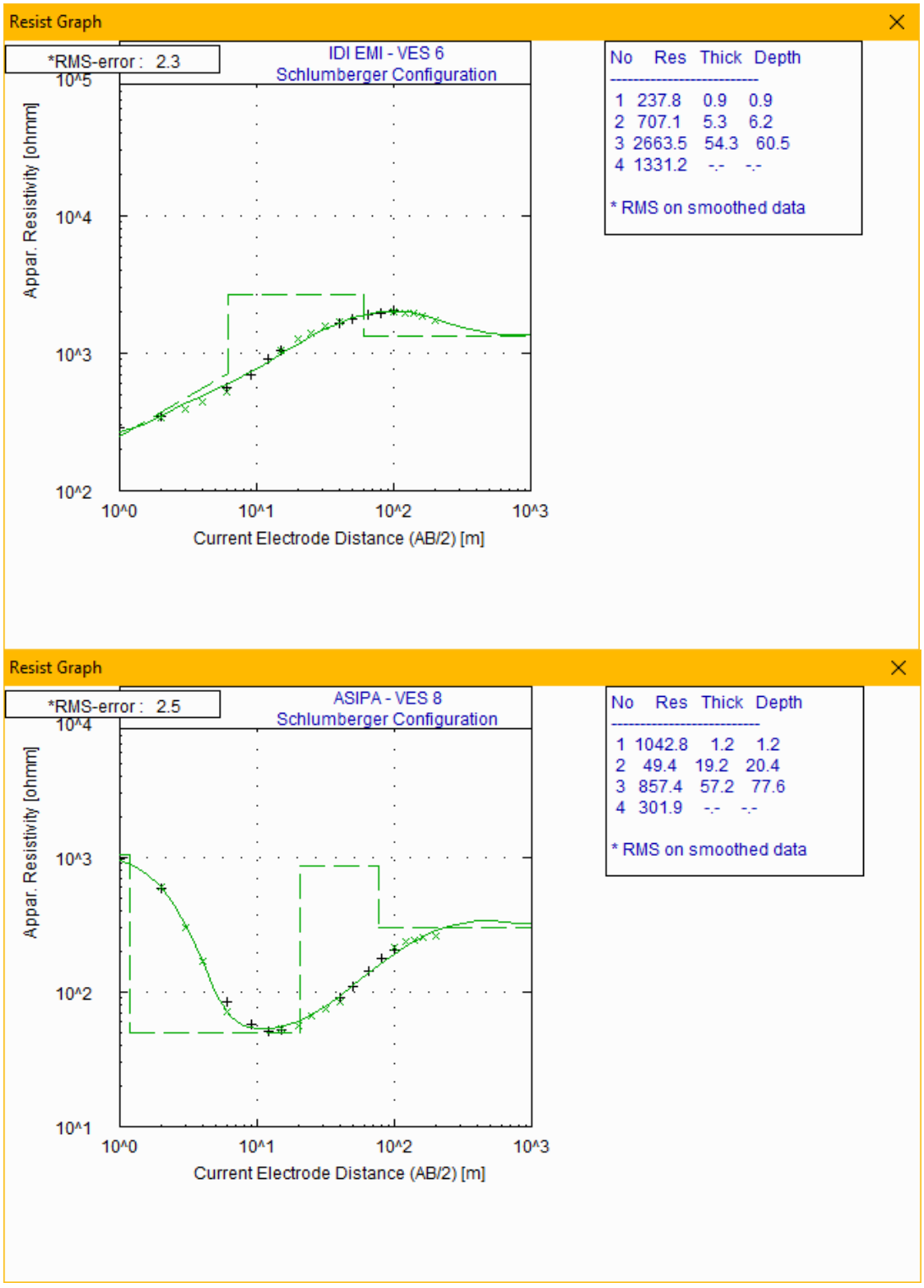

Figure. 4: a) Resistivity model for curve type AK b) resistivity model for curve type HK

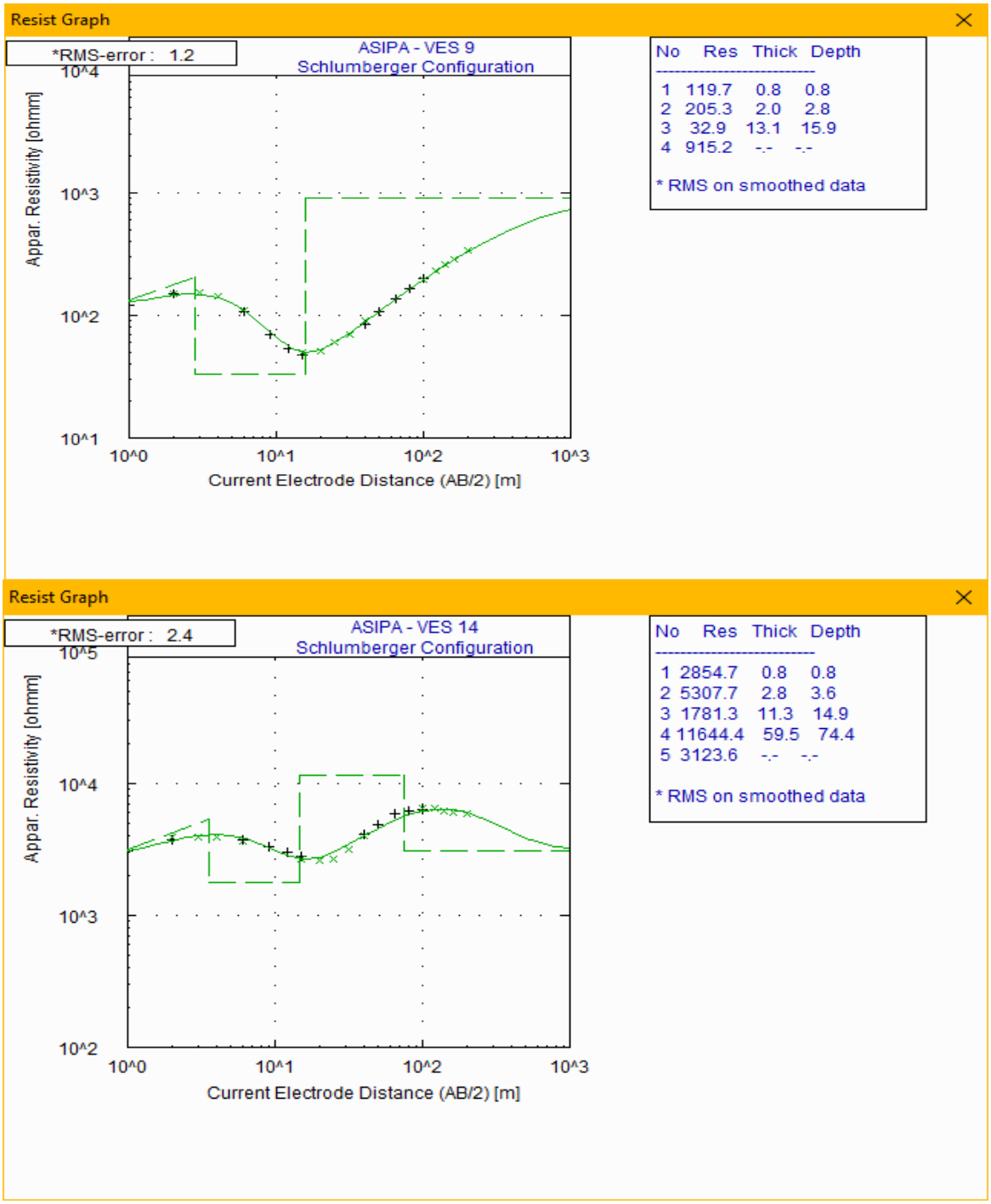

Figure. 5: a) Resistivity model for curve type KH b) resistivity model for curve type KHK

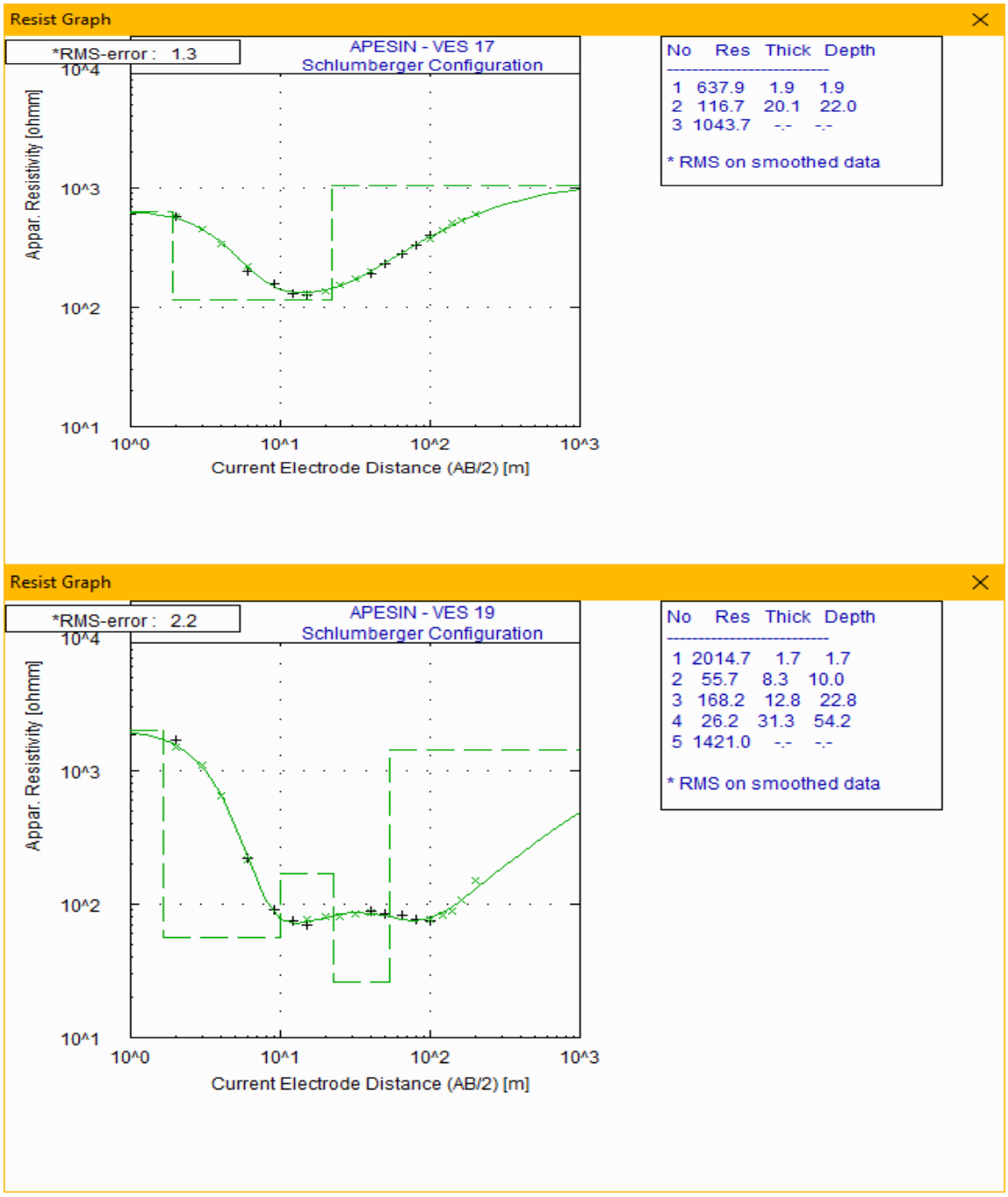

Figure. 6: a) Resistivity model for curve type H b) resistivity model for curve type HKH

Transition Zone

Geo-electric settings along Traverse 2 are marked by both lateral and vertical variation in geo-electric parameters. This traverse comprised of eight (8) correlated VES stations (VES 8, 9, 10, 11, 12, 13, 14 and 15), underlain by a range of four (4) – five (5) geo-electric layers. Depicted on Fig. 9 is the geo-electric section along traverse 2. This section is characterized by abrupt contrast in resistivity, thickness and orientation of geo-electric units. On the basis of these parameters, two broad geo-electric categorizations are recognized, which are, the obliquely warping northern portion and the thickly stratified southern segment, possessing a resistivity range of 33 Ωm – 1500 Ωm and 1894 Ωm – 11664 Ωm respectively.

Although four geo-electric layers are vertically revealed beneath the northern flank (VES 8, 9, 10, and 11), their correlation, however, revealed the presence of seven geo-electric units due apparently to the geologic complexity of this locality. The units from top to bottom ranges in resistivity between 120 Ωm – 1043 Ωm, 180 Ωm – 250 Ωm, 33 Ωm – 80 Ωm, 330 Ωm - 471 Ωm, 630 Ωm – 1500 Ωm and 302 Ωm (Fig. 9); which respectively correspond to the topsoil, lateritic clay, clay, clayey sand, fresh basement and fractured basement. The topsoil is laterally heterogeneous, consisting of sandy clay and sand. Its thickness range is 0.8 m – 1.2 m around this axis. Beneath the topsoil, lies the lateritic clay which ranges from 2.0 m – 4.2m in thickness. A thick descending clay unit, ranging between 13.1 m – 29.0 m underlies the laterite. Both the lateritic clay and clay units are obliquely inclined. Towards the central part of the traverse, the overburden became more progressively sandy (clayey sand composition) and nearly vertically descended (submerged). This submerged clayey sand unit is at least 48 m thick; extending to infinity basin-ward. Cumulatively, the overburden thickness ranges between 15.9 m to 58.0 m on the basement flank.

A very thick geo-electric sequence which rest unconformably on the clayey sand overburden occupies the southern half of the traverse. The stratum resistivity, from top to bottom, ranges from 1623 Ωm – 2855 Ωm, 3270 Ωm – 5513 Ωm, 1200 Ωm – 3900 Ωm, 3699 Ωm – 11664 Ωm and 1893 Ωm – 4244 Ωm; indicative of the topsoil, upper conglomeratic sand, kaolinitic sand, lower conglomeratic sand and sand respectively. With the exception of the basal sandstone with infinite thickness, thickness range of individual stratum is 0.8 m – 0.8 m, 2.4 m – 3.1m, 9.0 m – 15.1m, 38.5 m – 70.6 m in the aforementioned order. Inferred succession along the sedimentary segment revealed the preponderance of thick conglomeratic strata intercalating the sandstone strata. At the surface, the sequence is extensively capped by conglomeratic topsoil. This sequence, according to Omatsola and Adegoke (1981) is known as Ise formation. The formation occurs as a vast plateau landform around the Asipa axis.

Basement Terrain

Six resistivity curves (VES16, 17, 18, 19, 20 and 22) are recognized as basement curves, on the basis of resistivity relationships of the iterated parameters (Fig. 3-6). The basement territory is underlain by a range of three to five geo-electric layers. Areas underlain by three geo-electric layers (VES 17, 20 and 22) varied in resistivity value between 102 Ωm – 638 Ωm, 25 Ωm - 117 Ωm and 943 Ωm - 1500 Ωm from top to bottom; which is respectively indicative of topsoil, weathered layer (clay and sandy clay) and fresh basement. Topsoil ranges in thickness between 0.9 m – 1.9 m, weathered layer between 18.5 m – 22.5 m while the thickness of the fresh basement extends to infinity. However, depth range to the fresh basement interface is 15 m – 22 m.

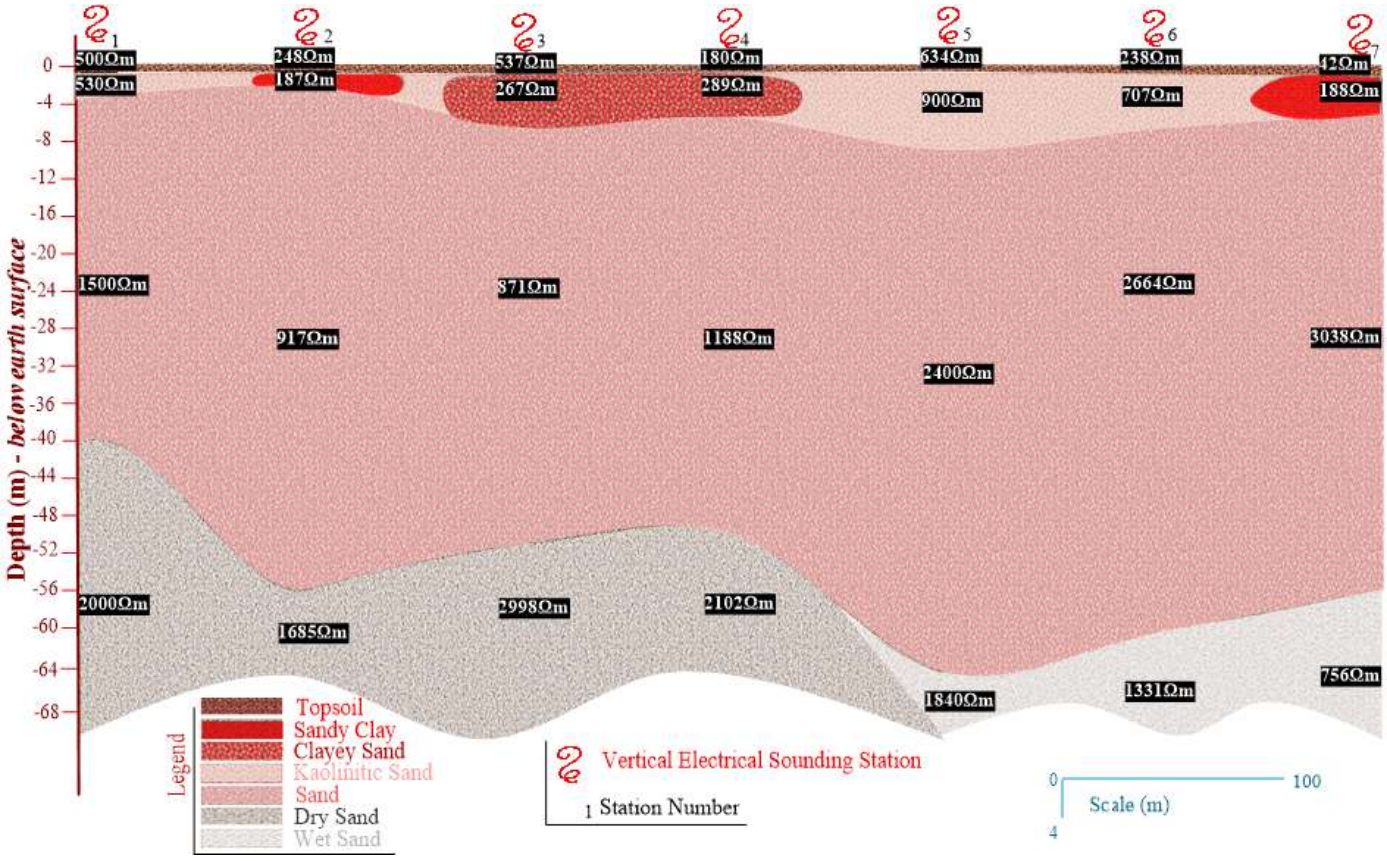

Figure . 7: Geo-electric Section along Traverse 1 which falls within Sedimentary Terrain, Idi Emi.

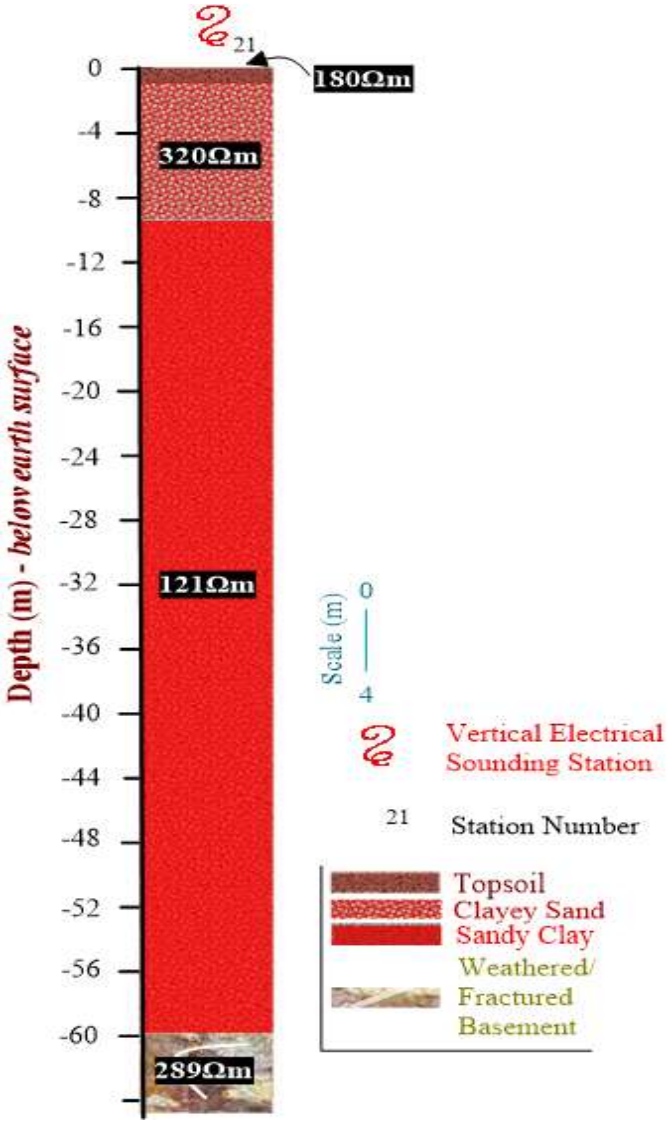

Figure. 8: Geo-electric Section of VES 21, Ogene Axis

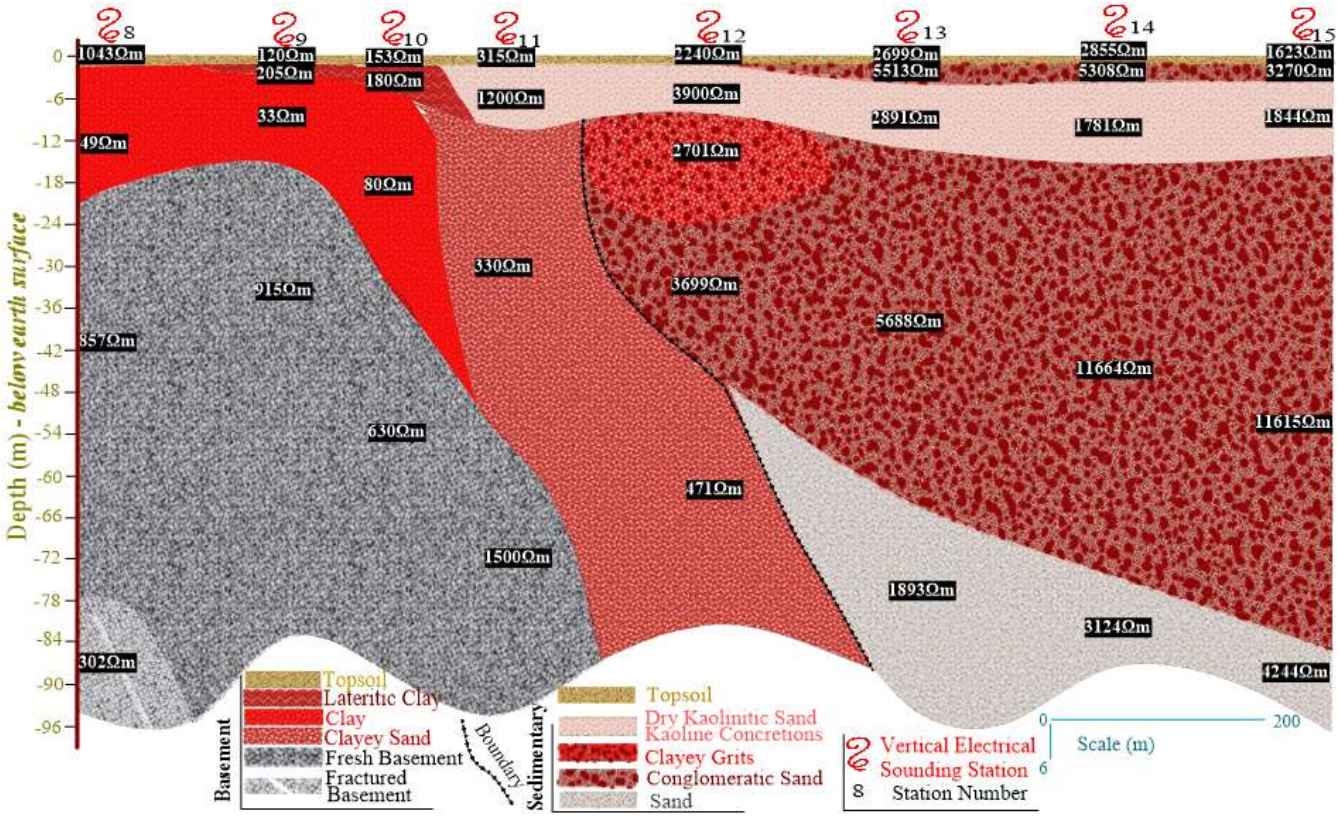

Figure. 9: Geo-electric Section along the Traverse 2, Idi-Emi Transition Zone

Four geo-electric units are surveyed beneath VES 16, 17, 18, 19, and 20. VES 16 is an HK curve that, from top to bottom, has a resistivity value of 1071 Ωm for topsoil, 59 Ωm for clay, 1231 Ωm for fresh basement, and 202 Ωm for fractured basement. The thickness of the topsoil, clay, and fresh basement are 1.1 m, 25.8 m, and 57.2 m, respectively, while the depth to the top of the fracture is 79.6 m. Logically, the depth to the fresh basement is 25.8 m (similar to that of a typical three-layer model), but the deeper presence of fractures within the basement rocks further created another geo-electric layer of anomalous resistivity.

VES stations 9, 10, and 11, on the other hand, revealed a KH signature. Resistivity value, from top to bottom, ranges between 120 Ωm – 315 Ωm, 180 Ωm – 1200 Ωm, 33 Ωm – 330 Ωm, and 915 Ωm – 1500, interpreted as the topsoil, lateritic clay/kaolinitic sand, clay/clayey sand, and fresh basement in that order. The corresponding thickness range is 0.8 m – 1.2 m, 2.0 m – 4.8 m, and 13.1 m – 29.0 m, while that of the fresh basement extends to infinity. Total overburden thickness covering the fresh basement ranges between 15.9 m and 58.0 m. In the case of a five-layered basement subsurface encountered beneath VES 18 and 19, the resistivity and thickness ranges of the five (5) geo-electric layers, from top to bottom, are 1105 Ωm – 2015 Ωm and 1.0 m – 1.7 m, 56 Ωm – 100 Ωm and 5.6 m – 8.6 m, 168 Ωm – 393 Ωm and 10.5 m – 12.8 m, 26 Ωm – 65 Ωm and 23.0 m – 31.3 m, and 1421 Ωm – 1602 Ωm with an infinite thickness. Lithologic inference in that order is topsoil, clay/sandy clay, sandy clay/clayey sand, fractured basement, and fresh basement. Depth to fresh basement ranges from 40.1 m to 54.2 m.

Subsurface cross-section of the basement curves (VES 16, 17, 18, 19, and 20) as a whole revealed a range of three to five geo-electric layers. Increments in geo-electric beyond three layers are due either to heterogeneity of the weathered basement or occurrences of fractures within the crystalline basement in this area. The geo-electric section along traverse 3 (Fig. 10) is apparently a depiction of three to five geo-electric layers, but the subsurface resistivity setting can be appropriately reclassified into four geo-electric layers, which from top to bottom ranges from 338 Ωm – 2015 Ωm, 56 Ωm – 393 Ωm, 26 Ωm – 202 Ωm, and 1044 Ωm – 2000 Ωm for topsoil, weathered layer, fractured basement, and fresh basement. The topsoil is 0.9 m – 1.9 m in thickness. Thickness of the weathered layer varied between 15.0 m and 26.9 m. On the basis of depth occurrence, two fractured zones are recognized, which are the upper and lower basement fractures (Fig. 10).

The upper fractured basement is a 23.0 m – 31.3 m thick conductive zone whose depth never exceeded 55 m. The lower fractured basement, on the other hand, is a relatively deeper fractured zone, occurring below 80.0 m depth. Depth to the fresh basement varied between 15.0 m and 54.2 m around the upper fractured zone. However, vicinities underlain by lower fractured basement exhibit a dual interface with the fresh basement—the upper interface bounded by regolith but the lower by the fractures. Depth of the regolith cover on the fresh basement ranges between 15.0 m and 26.9 m.

Fig. 11 is the geo-electric log beneath VES 22, stationed around the Obada axis. It is underlain by three geo-electric layers, which, from top to bottom, are characterized by a

resistivity and thickness of 104 Ωm and 1.4 m (inferred as topsoil), 25 Ωm and 17.1 m (clay), and 943 Ωm (fresh basement). Apesin and Obada axes are two prominent basement localities with typical undulating depth-to-basement ranges, which generally varied between 18.5 m and 26.9 m. Around fractured basement provinces, however, the depth is deeper, ranging between 40.1 m and 54.2 m beneath the shallow fractured zones but definitely far below 80 m underneath the deeper fractures.

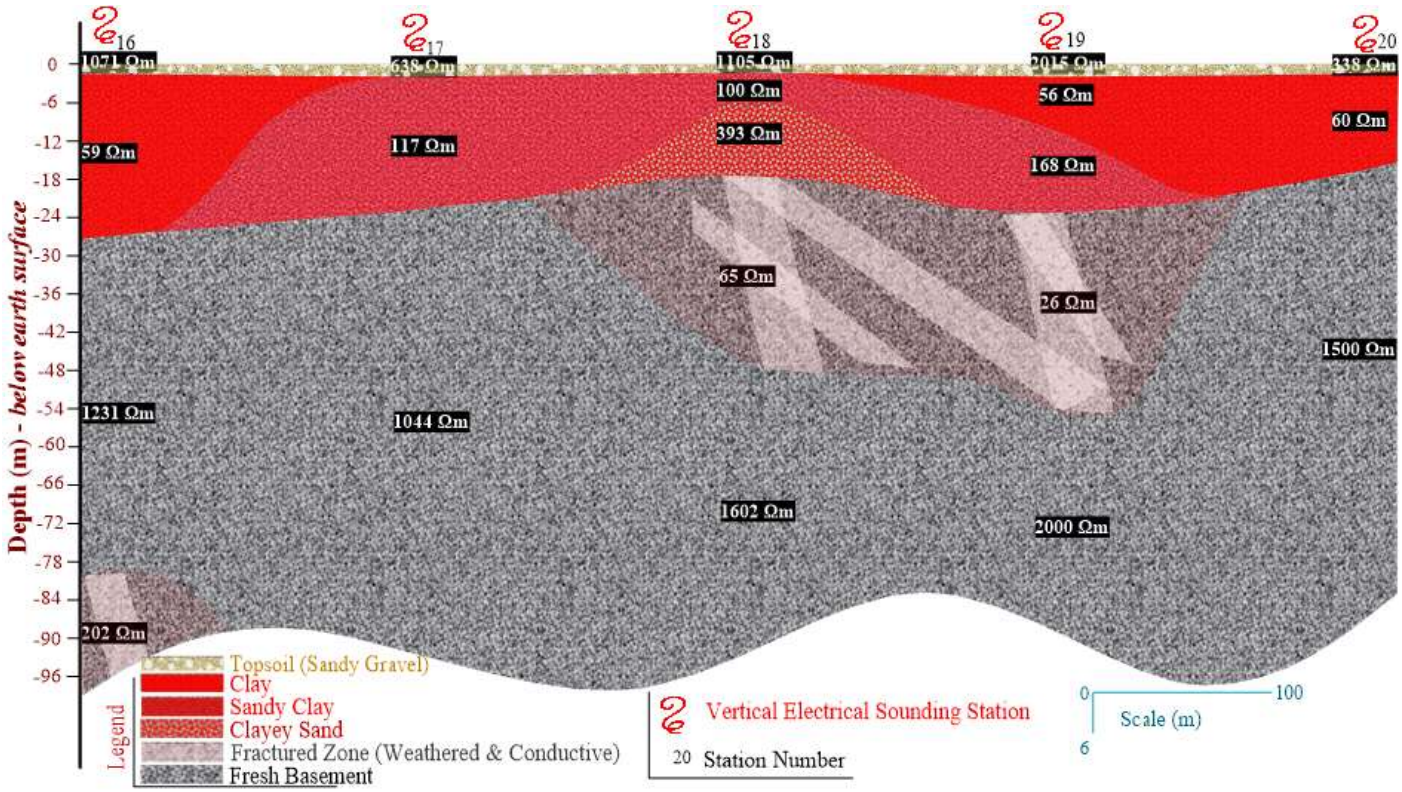

Figure. 10: Geo-electric Section along Traverse 3. This traverse falls within the Basement Terrain.

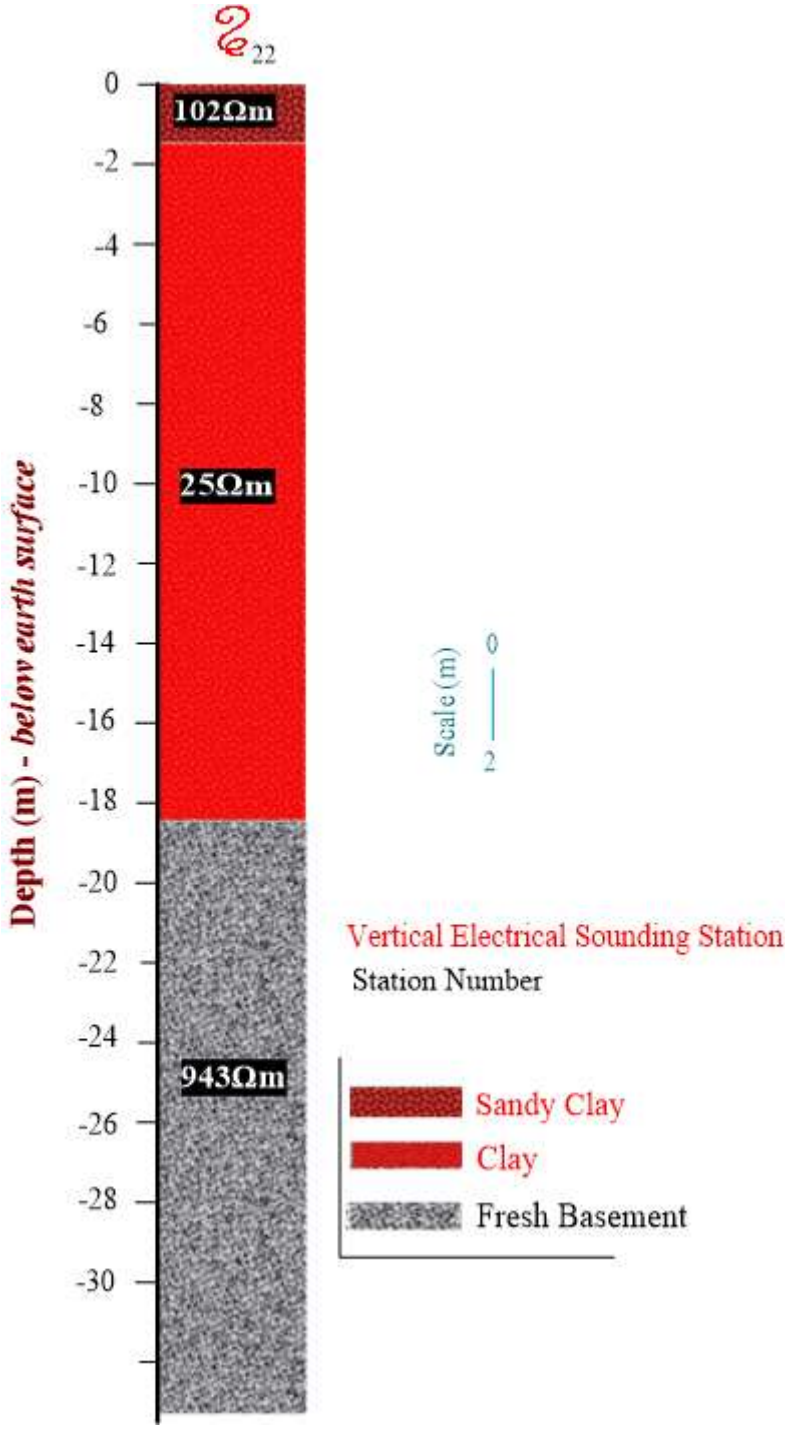

Figure. 11: Geo-electric Section of VES 22, revealing Obada Axis as a Basement Territory.

A. Geologic Boundary Delineation

A very accurate geologic boundary (Fig. 12) has been drawn from both geological evidence and geophysical results. The basement complex roughly covers about three-quarters of the area map, occupying the northern and southeastern parts. Localities covered include Apesin, Ojubu, Asipa, and parts of Obada. Sedimentary terrain only accounts for about one-quarter of the area map. These rocks are dominant in the southwestern part of the area, notably around the Idi-Emi and Obada axes.

There is a strong link between the physiographic settings and geology of the area. Sedimentary terrain, due to a massive influx of sediment, is distinctively higher in elevation than the basement. It functions as the main watershed from which the rivers take their sources. The drainage pattern is fairly dendritic with a resultant northeasterly flow into the basement. Along the sedimentary escarpments, a thick sequence of ferruginized conglomerate or conglomeratic sand with kaolinitic interbeds is exposed. A few tens to hundreds of meters away from the escarpment, the weathered basement was encountered. The escarpment is thus not only a

topographic marker but also a fairly accurate geologic pointer to the existence of a nearby nonconformity.

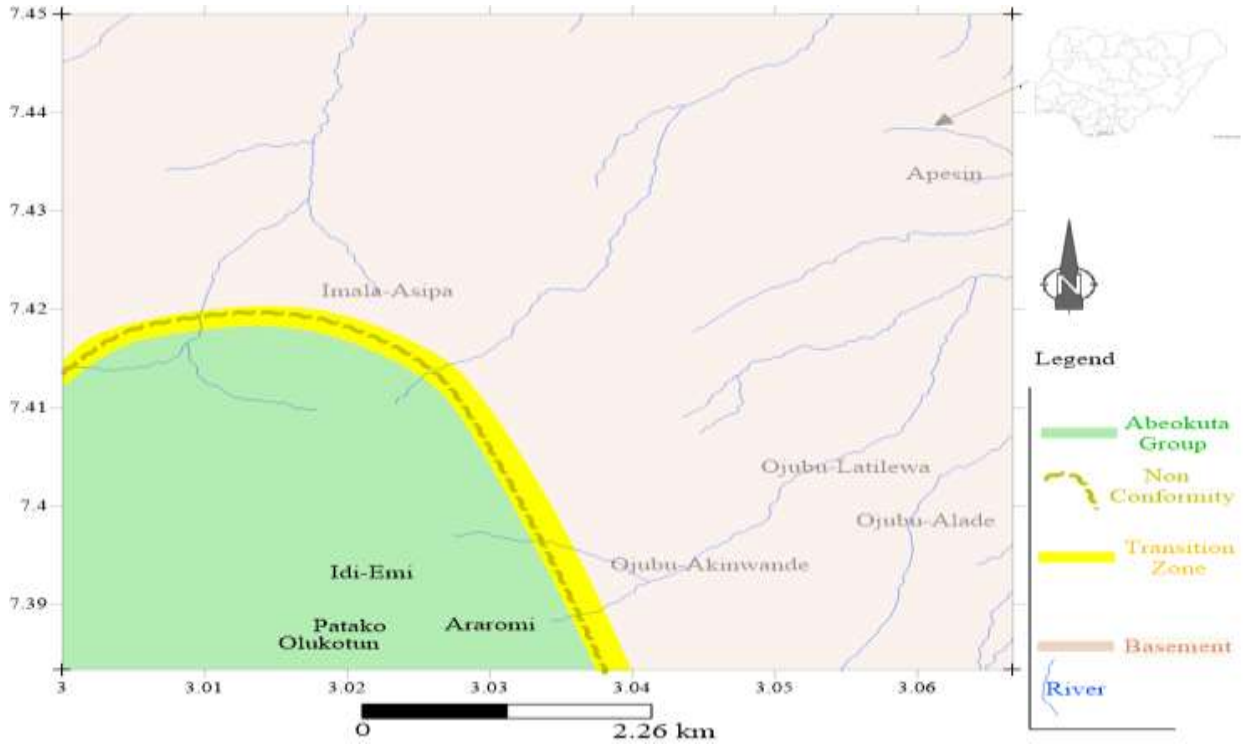

Figure. 12: Inferred Geologic Map of the Study Area Revealing the Basement – Sedimentary Contact.

V. CONCLUSION

The study employed the VES and 2D electrical resistivity method to characterize the subsurface of the study area into geo-electric sections, determining the depth to the basement and delineating possible zones that can serve as unique rocks from the various anomalous zones. The investigation revealed new geological boundaries within sedimentary areas, crystalline basement, and transition zones. This result provides a modern geological map of Idi-Emi that is consistent with the recent regional geological map of the Dahomey Basin. From the geophysical results and inferences, the Apesin and Obada axes are essentially part of the Nigerian Basement complex, while the Idi-Emi in the southern part is wholly sedimentary. The boundary line between these two geologic provinces is delineated at the Imala, Asipa, and Ogene axes. The study area is thus a transition zone bearing the imprints of both the basement and the sedimentary environments. Lastly, defining the boundary between the basement complex and sedimentary terrain aids in determining where different rock types and formations occur. The refined delineation of lithological zones and basement depths in the Idi-Emi area enhances the identification and management of groundwater potential, crucial for sustainable water resource development. Furthermore, the detailed resistivity and thickness data support engineering site investigations by informing the stability and suitability of the ground for construction and infrastructure projects. Additionally, the improved geological mapping aids environmental management efforts by helping to monitor and control illegal mining activities, thereby promoting safer land-use planning and resource conservation.

REFERENCES

[1] P. V. Sharma, Geophysical methods in geology., 2nd Edition ed., U.S. Department of Energy, 1985.

[2] K. Wattanasen, S. Å. Elming, W. Lohawijarn and T. and Bhongsuwan, "An integrated geophysical study of arsenic contaminated area in the peninsular Thailand," *Environmental geology,* vol. 51, no. 4, pp. 595 - 608, 2006.

[3] S. A. Adekoya, H. T. Oladunjoye, J. O. Coker, O. A. Adenuga and G. O. Badmus, "Groundwater exploration and evaluation of aquifer vulnerability in parts of main campus of Olabisi Onabanjo University Southwestern Nigeria," *FUW Trends in Science & Technology Journal,* vol. 9, no. 1, pp. 271-277, 2024.

[4] S. A. Adekoya, J. O. Coker, H. T. Oladunjoye and O. A. Adenuga, "Aquifer characterization of some parts of Ijebu Igbo using electrical resistivity methods," in *Journal of Physics: Conference Series*, 2019.

[5] J. C. Wynn, "A review of geophysical methods used in archaeology," *Geoarchaeology,* vol. 1, no. 3, pp. 245-257., 1986.

[6] C. F. Gaffney, J. Gater and S. Ovenden, *The use of geophysical techniques in archaeological evaluations.,* 2002.

[7] A. F. Abimbola, O. O. Kehinde-Phillips and A. S. Olatunji, "The Sagamu cement factory, SW Nigeria: Is the dust generated a potential health hazard?," *Environmental geochemistry and health,* vol. 29, no. 2, pp. 163-167., 2007.

[8] S. O. Ariyo, K. O. Omosanya and B. A. Oshinloye, "Electrical resistivity imaging of contaminant zone at Sotubo dumpsite along Sagamu-Ikorodu Road, Southwestern Nigeria," *African Journal of Environmental Science and Technology,* vol. 7, no. 5, pp. 312-320, 2013.

[9] O. I. Popoola and O. A. Adenuga, "Determination of leachate curtailment capacity of selected dumpsites in Ogun State southwestern Nigeria using integrated geophysical methods," *Scientific African,* vol. 5, p. e00208., 2019.

[10] M. B. Aminu, "Electrical resistivity imaging of a thin clayey aquitard developed on basement rocks in parts of Adekunle Ajasin University Campus, Akungba-Akoko, South-western Nigeria," *Environmental Research, Engineering and Management,* vol. 71, no. 1, pp. 47-55, 2015.

[11] C. E. Bond, "Uncertainty in structural interpretation: Lessons to be learnt.," *Journal of Structural Geology,* vol. 74, p. 185–200, 2015.

[12] G. O. Mosuro, N. O. Adebisi, S. O. Ariyo, K. O. Omosanya, O. O. Bayewu and M. O. Oloruntola, "Redefining the boundary between crystalline and sedimentary rock of Eastern Dahomey Basin," *Scientific reports,* vol. 11, no. 1, pp. 1-15., 2021.

[13] P. Ramaekers, C. W. Jefferson, G. M. Yeo, B. Collier, D. G. F. Long, G. Drever and R. T. Post, "Revised geological map and stratigraphy of the Athabasca Group, Saskatchewan and Alberta," *Bulletin-Geological Survey of Canada,* vol. 588, p. 155, 2007.

[14] E. D. Ashaolu and K. A. Iroye, "Rainfall and potential evapotranspiration patterns and their effects on climatic water balance in the Western Lithoral Hydrological Zone of Nigeria," *Ruhuna Journal of Science,* vol. 9, no. 2, 2018.

[15] S. A. Adekoya, H. T. Oladunjoye, J. O. Coker and O. A. Adenuga, "Identification of lithological units using geo-electrical method, Olabisi Onabanjo University Campus, Southwestern Nigeria.," *Scientia Africana,* vol. 20, no. 1, pp. 171-182, 2021.

[16] J. A. Aladejana and A. O. Talabi, "Assessment of groundwater quality in Abeokuta Southwestern, Nigeria," *International Journal of Engineering Science,* vol. 2, no. 6, pp. 21-31, 2013.

[17] V. Makinde, S. A. Ganiyu, B. S. Bada, A. O. Salawu, O. A. Ifeyemi and J. O. Odutayo, "Hydrogeophysical exploration and groundwater quality assessment of Obada Oko, Ogun State, Nigeria," *Ife Journal of Science,* vol. 26, no. 3, pp. 737-755, 2024.

[18] A. A. Kayode, "Charnockitic Hypersthene-Quartz Diorite from Imala, Southwestern Nigeria," *Journal of Geological Society of India,* vol. 17, no. 1, pp. 54-60, 1976.

[19] T. Dahlin and B. Zhou, "A numerical comparison of 2D resistivity imaging with 10 electrode arrays.," *Geophysical Prospecting,* vol. 52, no. 5, pp. 379-398, 2004.

[20] M. H. Loke, " Tutorial: 2D and 3D Electrical Imaging Surveys," Geotomo Software, 2019.

[21] B. D. Ako and M. O. Olorunfemi, "Geoelectric survey for groundwater in the new layout of Ile-Ife, Nigeria.," *Journal of Mining and Geology,,* vol. 25, no. 1-2, p. 247–250, 1989.

[22] A. I. Olayinka and M. O. Olorunfemi, "Determination of geoelectrical characteristics in Okene area and implications for borehole siting," *Journal of African Earth Sciences,* vol. 14, no. 3, p. 329–337, 1992.

[23] N. G. Obaje, Geology and mineral resources of Nigeria, vol. 120, Berlin: Springer, 2009, p. 221.

[24] R. R. Jones, K. J. W. McCaffrey, P. Clegg, R. W. Wilson, N. S., R. Holliman, J. Holdsworth, J. Imber and S. Waggott, "Integration of regional to outcrop digital data: 3D visualisation of multi-scale geological models," *Computers & Geosciences,* vol. 35, no. 1, pp. 4-8, 2009.

[25] C. Mitchell and M. Widdowson, "A geological map of the southern Deccan Traps, India and its structural implications.," *Journal of the Geological Society, ,* vol. 148, no. 3, pp. 495-505, 1991.